

Intense Yellow Emission from $\text{Gd}_{0.5-y}\text{Tb}_{1.5}\text{RE}_y\text{W}_3\text{O}_{12}$ (RE=Eu, Sm) Phosphors Tuned through Full Range Doping

DAI Yan-Nan¹, YANG Shuai¹, SHEN Yang², SHAN Yong-Kui¹, YANG Fan¹, ZHAO Qing-Biao²

(1. School of Chemistry and Molecular Engineering, East China Normal University, Shanghai 200241, China; 2. Key Laboratory of Polar Materials and Devices (MOE), Department of Optoelectronics, East China Normal University, Shanghai 200241, China)

Abstract: Yellow emission phosphors play an important role in fabrication of near ultraviolet (NUV) chip pumped white light emitting diodes (W-LEDs). In this study, doping of $\text{Gd}_2\text{W}_3\text{O}_{12}$ host with Tb^{3+} and $\text{Eu}^{3+}/\text{Sm}^{3+}$ were used for obtaining yellow light emission. The excitation of Gd^{3+} typically is in deep ultraviolet region, but Gd^{3+} in $\text{Gd}_2\text{W}_3\text{O}_{12}$ does not emit under the excitation of 382 nm, thus Gd^{3+} does not interfere with the emission from Tb^{3+} and $\text{Eu}^{3+}/\text{Sm}^{3+}$ for obtaining yellow emission. Due to the similar ionic radii, the doping of Gd^{3+} by Tb^{3+} can be achieved in the full concentration range, and at the optimal concentration of 75mol% Tb^{3+} , green emission with reasonably high internal quantum efficiency of 37.6% was obtained. With the optimal doping concentration of Tb^{3+} , $\text{Eu}^{3+}/\text{Sm}^{3+}$ was co-doped in the $\text{Gd}_2\text{W}_3\text{O}_{12}$ host, and bright yellow emission with IQE of 39.6% and 47.8% were obtained. The yellow phosphors of $\text{Gd}_{0.494}\text{Tb}_{1.5}\text{Eu}_{0.006}\text{W}_3\text{O}_{12}$ and $\text{Gd}_{0.494}\text{Tb}_{1.5}\text{Sm}_{0.006}\text{W}_3\text{O}_{12}$ were used to fabricate W-LED devices with NUV-blue chips. Thus, $\text{Gd}_{0.5-y}\text{Tb}_{1.5}\text{RE}_y\text{W}_3\text{O}_{12}$ (RE=Eu, Sm) phosphors are candidates as the yellow phosphors for fabricating W-LED devices. Additionally, the full-range doping strategy can be used in other systems for obtaining efficient phosphors.

Key words: solid state synthesis; photoluminescence; tungstate; rare earth; internal quantum efficiency

White light emitting diodes (W-LEDs) have received much attention for their high efficiency, long service life and small volume^[1-3]. There are primarily three approaches for obtaining W-LEDs, including tri-color (red, green, blue) diode chips^[4], blue chips coated with yellow phosphors^[5], and ultraviolet (UV) chips coated with RGB phosphors^[6]. The LED chips used for solid state lighting can typically provide near ultraviolet (NUV) excitation in the region of 380–420 nm. Therefore, the phosphors that can be efficiently excited in this region are desired.

The commercialized cerium (III)-doped yttrium aluminum garnet (YAG: Ce^{3+}) emit strong yellow light under blue excitation from InGaN chips^[7]. Besides, some other novel Ce^{3+} doped phosphors with high quantum efficiency had been reported in recent years^[8-9]. However, the preparation of Ce^{3+} doped phosphors requires a reducing atmosphere, which inevitably adds to the cost. Moreover, Ce^{3+} tends to be oxidized to the tetravalent state if exposed to air. Thus, it is desired to develop new phosphors that can be prepared in ambient atmosphere. Yellow light can be obtained by adjusting the ratio of

green light to red light. Tb^{3+} and Eu^{3+} (or Sm^{3+}) ions can be excited by NUV, emit green and red light, respectively^[10-11]. Therefore, it is possible to realize yellow light emission under NUV excitation by adjusting the doping ratio of $\text{Tb}^{3+}/\text{Eu}^{3+}$ or $\text{Tb}^{3+}/\text{Sm}^{3+}$ in proper hosts.

Rare earth ion based tungstates have drawn increasing attention for their low phonon energy and high thermal stability^[12-13]. Since the electronic configuration of Gd^{3+} ($4f^7$) is half full, the f-f transition ($^8\text{S}_{7/2} \rightarrow ^6\text{I}_J$) of Gd^{3+} generally takes place at deep ultraviolet region, and Gd^{3+} generally does not exhibit emission in visible range^[14]. $\text{Gd}_2\text{W}_3\text{O}_{12}$ can provide suitable substitution sites for rare earth ions, thus can function as the host of rare earth ion doped phosphors. As the ionic radius of Tb^{3+} , Eu^{3+} and Sm^{3+} are very close to that of Gd^{3+} ^[15], those rare earth ions were introduced to substitute the positions of Gd^{3+} ions in $\text{Gd}_2\text{W}_3\text{O}_{12}$. The substitution of Gd^{3+} by Tb^{3+} can perform in the entire range, allowing the fine tuning of the optimal doping rate in order to obtain the maximum IQE for the green emission. Eu^{3+} and Sm^{3+} ions can be efficiently excited by NUV/blue light and emit in the red range^[16-17]. With the combination of green emission from

Received date: 2018-11-08; Modified date: 2019-01-29

Foundation item: The Startup Funding of East China Normal University (11200-120215-10363)

Biography: DAI Yan-Nan(1993–), female, candidate of Master degree. E-mail: 51164300103@stu.ecnu.edu.cn

Corresponding author: YANG Fan, professor. E-mail: fyang1@chem.ecnu.edu.cn; ZHAO Qing-Biao, professor. E-mail: qbzha@ee.ecnu.edu.cn

Tb^{3+} and red emission from $\text{Eu}^{3+}/\text{Sm}^{3+}$, co-doping Eu^{3+} (or Sm^{3+}) with Tb^{3+} is another strategy for obtaining yellow emission, which does not require reducing environment.

In this study, the photoluminescence properties of Eu^{3+} (or Sm^{3+}) and Tb^{3+} co-doped $\text{Gd}_2\text{W}_3\text{O}_{12}$ phosphors with yellow light emission are reported. The IQE of $\text{Gd}_{0.494}\text{Tb}_{1.5}\text{Eu}_{0.006}\text{W}_3\text{O}_{12}$ and $\text{Gd}_{0.494}\text{Tb}_{1.5}\text{Sm}_{0.006}\text{W}_3\text{O}_{12}$ are 39.6% and 47.8%, respectively. Furthermore, they can be synthesized under ambient atmosphere, thus avoiding the requirement of reducing atmosphere. $\text{Gd}_{0.494}\text{Tb}_{1.5}\text{Eu}_{0.006}\text{W}_3\text{O}_{12}$ and $\text{Gd}_{0.494}\text{Tb}_{1.5}\text{Sm}_{0.006}\text{W}_3\text{O}_{12}$ are promising candidates for yellow phosphors. The full-range doping approach can be used in search for novel phosphors with high efficiency.

1 Experimental

A series of $\text{Gd}_2\text{W}_3\text{O}_{12}$: Tb^{3+} , Eu^{3+} (or Sm^{3+}) phosphors were synthesized by traditional high temperature solid state synthesis. The starting materials of Tb_4O_7 (Adamas Reagent, 99.99%), WO_3 (Adamas Reagent, 99.90%), Gd_2O_3 (Adamas Reagent, 99.99%), Eu_2O_3 (Adamas Reagent, 99.90%) and Sm_2O_3 (Adamas Reagent, 99.90%) were weighed in stoichiometric ratio and thoroughly ground in an agate mortar. After thoroughly mixing, the reactants were transferred to an alumina crucible and heated at 600 °C for 8 h. After cooling to room temperature, the obtained intermediate products were re-ground and calcined at 1000 °C for 24 h.

The XRD patterns were collected by a Bruker D8 diffractometer with $\text{CuK}\alpha$ ($\lambda=0.154059$ nm) radiation at 40 kV and 40 mA. The excitation and emission spectra of $\text{Gd}_2\text{W}_3\text{O}_{12}$: Tb^{3+} , Eu^{3+} (or Sm^{3+}) phosphors were collected with a Hitachi F4500 Fluorometer. The internal quantum efficiencies (IQE) were measured by Edinburgh (EI) FS5 fluorometer equipped with an integrating sphere. The IQE was calculated with equation (1):

$$\eta = \frac{E_B - E_A}{S_A - S_B} \times 100\% = \frac{\int E_B(\lambda) d\lambda - \int E_A(\lambda) d\lambda}{\int S_A(\lambda) d\lambda - \int S_B(\lambda) d\lambda} \times 100\% \quad (1)$$

where E_B is the emission integral of the sample, E_A is the emission integral of the blank stander, S_A is the absorption integral of the blank stander and S_B is the absorption integral of the sample. A polytetrafluoroethylene plate was used as the reference.

2 Results and discussion

2.1 Structural analysis

$\text{Gd}_{2-x}\text{W}_3\text{O}_{12}$: $x\text{Tb}^{3+}$ ($x = 0, 0.25, 0.75, 1.00, 1.25, 1.50, 1.75, 2.00$) phosphors were synthesized by high temperature solid state synthesis. The crystal structures of

$\text{Tb}_2\text{W}_3\text{O}_{12}$ and $\text{Gd}_2\text{W}_3\text{O}_{12}$ have been reported^[18]. The crystal structure of the as-prepared $\text{Gd}_2\text{W}_3\text{O}_{12}$ belongs to the monoclinic system. The space group is C2/c with the following lattice parameters: $a=0.7811$ nm, $b=1.1629$ nm, $c=1.1537$ nm, $\alpha=\gamma=90^\circ$, $\beta=109.719^\circ$. In $\text{Gd}_2\text{W}_3\text{O}_{12}$, each Gd atom is coordinated with 8 O atoms, forming a $[\text{GdO}_8]$ polyhedron without inversion center. As shown in Fig. 1(a, b), each $[\text{GdO}_8]$ polyhedron shares one side with two nearest $[\text{GdO}_8]$ polyhedron. Thus a one-dimensional chain structure is formed, which plays an important role for the high concentration quenching of Tb^{3+} in $\text{Gd}_2\text{W}_3\text{O}_{12}$.

Fig. 2 shows the XRD patterns of $\text{Gd}_2\text{W}_3\text{O}_{12}$, $\text{TbGdW}_3\text{O}_{12}$ and $\text{Tb}_2\text{W}_3\text{O}_{12}$, which are consistent with the JPCDS card of $\text{Gd}_2\text{W}_3\text{O}_{12}$ (JPCDS #23-1076). The cell parameters of $\text{Tb}_2\text{W}_3\text{O}_{12}$, $\text{Gd}_2\text{W}_3\text{O}_{12}$ only have a minor difference, and the crystal structure of $\text{Tb}_2\text{W}_3\text{O}_{12}$ and $\text{Gd}_2\text{W}_3\text{O}_{12}$ are similar. Therefore, the doping ratio of Tb^{3+} ions in $\text{Gd}_2\text{W}_3\text{O}_{12}$ can range from 0 to 100mol%.

The ionic radii of both Sm^{3+} (CN=8, $r=0.1079$ nm) and Eu^{3+} (CN=8, $r=0.1066$ nm) ions are also similar to Gd^{3+} (CN=8, $r=0.105$ nm) ions^[15]. Therefore, co-doping of Sm^{3+} or Eu^{3+} in Tb^{3+} doped $\text{Gd}_2\text{W}_3\text{O}_{12}$ is feasible. Apparently, in order to obtain yellow emission, doping on the Gd^{3+} site has a unique advantage in that both the doping ratios of Tb^{3+} as the green emission source and the doping ratios of $\text{Eu}^{3+}/\text{Sm}^{3+}$ as the red emission source can be tuned in a broad range. This allows fine tuning of both the overall emission wavelengths and emission intensity.

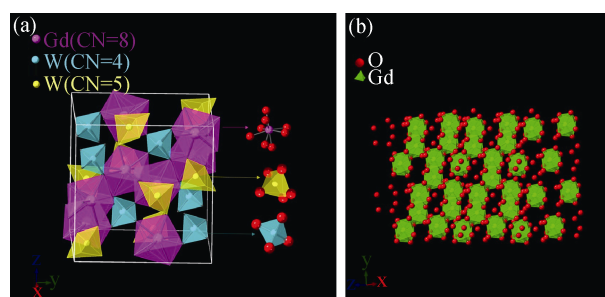


Fig. 1 (a) The polyhedron models of the crystal structure of $\text{Gd}_2\text{W}_3\text{O}_{12}$ from perspectives of x axis, (b) the one-dimensional chain structure of $[\text{GdO}_8]$ polyhedrons

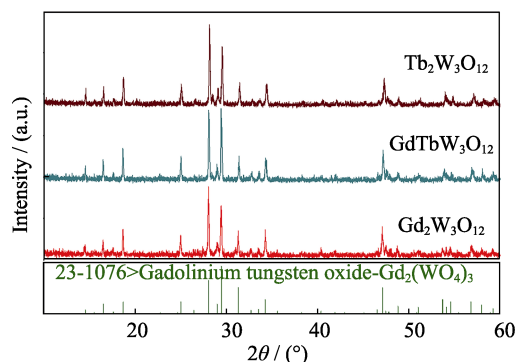


Fig. 2 XRD patterns of $\text{Gd}_2\text{W}_3\text{O}_{12}$, $\text{TbGdW}_3\text{O}_{12}$ and $\text{Tb}_2\text{W}_3\text{O}_{12}$

2.2 Luminescence property

Fig. 3(a, b) show the excitation spectra of $\text{Gd}_{2-x}\text{W}_3\text{O}_{12}: x\text{Tb}^{3+}$ phosphors monitored with 549 nm emission and the concentration dependent excitation intensity, respectively. There is a broad excitation band shorter than 320 nm which belongs to the charge transfer (CT) between W and O. The excitation at 321 nm ($^7\text{F}_6 \rightarrow ^5\text{D}_0$), 342 nm ($^7\text{F}_6 \rightarrow ^5\text{D}_1$), 361 nm ($^7\text{F}_6 \rightarrow ^5\text{D}_2$), 372 nm ($^7\text{F}_6 \rightarrow ^5\text{D}_3$), and 382 nm ($^7\text{F}_6 \rightarrow ^5\text{D}_4$) belong to the f-f transition of Tb^{3+} ions^[19]. With increasing concentration of Tb^{3+} ions up to 75mol% (when $x=1.50$), the excitation intensity gradually enhances. As the concentration of Tb^{3+} ions continue to increase, the excitation intensity gradually decreases. With Gd^{3+} ions entirely replaced by Tb^{3+} ions, $\text{Tb}_2\text{W}_3\text{O}_{12}$ shows a weak excitation.

Fig. 4 (a, b) show the emission spectra at 382 nm excitation and the concentration dependent emission intensities of $\text{Gd}_{2-x}\text{W}_3\text{O}_{12}: x\text{Tb}^{3+}$ ($x=0.25, 0.75, 1.00, 1.25, 1.50, 1.75, 2.00$) phosphors. The sharp peaks at 485, 549, 575 and 610 nm correspond to the relaxation processes ($^5\text{D}_4 \rightarrow ^7\text{F}_6$, $^5\text{D}_4 \rightarrow ^7\text{F}_5$, $^5\text{D}_4 \rightarrow ^7\text{F}_4$ and $^5\text{D}_4 \rightarrow ^7\text{F}_3$) of Tb^{3+} ions, respectively^[20]. As shown in Fig. 4 (a, b), with the doping amount of Tb^{3+} ions increasing to 75mol% ($x=1.50$), the emission intensity at 549 nm gradually increases, and the IQE of $\text{Tb}_{1.5}\text{Gd}_{0.5}\text{W}_3\text{O}_{12}$ enhances to 37.6%. The emission intensity at 549 nm gradually decreases with

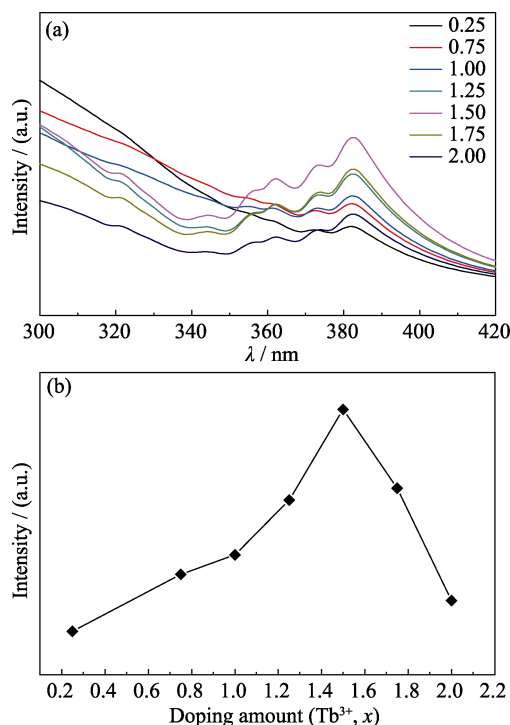


Fig. 3 (a) The excitation spectra of $\text{Gd}_{2-x}\text{W}_3\text{O}_{12}: x\text{Tb}^{3+}$ ($x=0.25, 0.75, 1.0, 1.25, 1.5, 1.75, 2.00$) monitored with 549 nm emission; (b) The concentration dependent excitation intensity of $^7\text{F}_6 \rightarrow ^5\text{D}_4$ transition of Tb^{3+} at 382 nm in $\text{Gd}_{2-x}\text{W}_3\text{O}_{12}: x\text{Tb}^{3+}$ (a) Coloful spectra are available on website

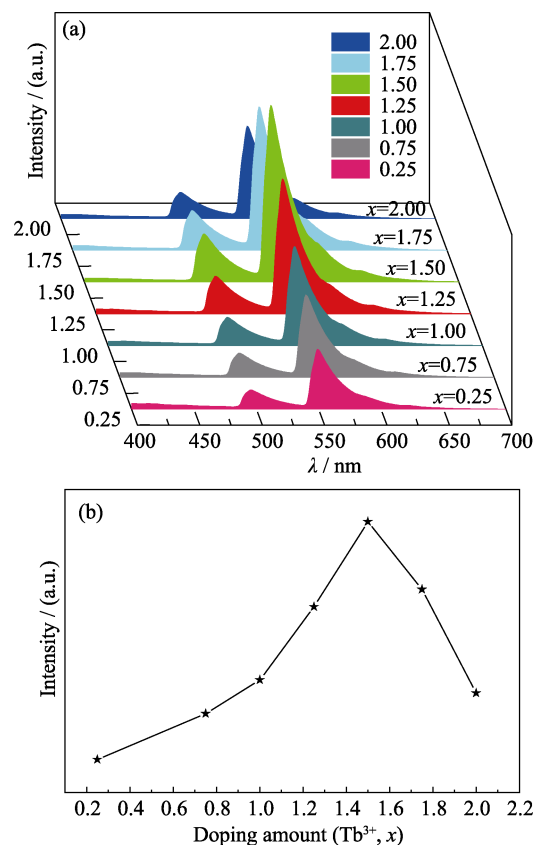


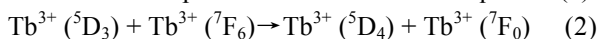
Fig. 4 (a) The emission spectra of $\text{Gd}_{2-x}\text{W}_3\text{O}_{12}: x\text{Tb}^{3+}$ ($x=0.25, 0.75, 1.00, 1.25, 1.50, 1.75, 2.00$) phosphors under 382 nm ultraviolet excitation; (b) The concentration dependent 549 nm emission intensity of $\text{Gd}_{2-x}\text{W}_3\text{O}_{12}: x\text{Tb}^{3+}$ (where $x=0.25, 0.75, 1.00, 1.25, 1.50, 1.75, 2.00$) phosphors

further increasing of the doping amount of Tb^{3+} . With the full occupancy of Tb^{3+} , the concentration quenching is significant and the emission intensity of $\text{Tb}_2\text{W}_3\text{O}_{12}$ is very weak, and the IQE of $\text{Tb}_2\text{W}_3\text{O}_{12}$ is only 12.6%.

The concentration quenching of Tb^{3+} doped $\text{Gd}_2\text{W}_3\text{O}_{12}$ occurs at a rather high concentration of 75mol%. Typically, the optimal doping concentration of rare earth activators for luminescence is in the range of 1mol%–20mol%. Realizing very high quenching concentration can be a strategy for realizing bright green emission.

It is intriguing to figure out the cause for the high concentration quenching of Tb^{3+} doped $\text{Gd}_2\text{W}_3\text{O}_{12}$. The mechanism of self-concentration quenching (SCQ) of Tb^{3+} and Eu^{3+} ions in $\text{LaMgB}_5\text{O}_{10}$ have been reported^[21]. Since edge-sharing $[\text{LaO}_{10}]$ polyhedron in $\text{LaMgB}_5\text{O}_{10}$ form isolate chains, one-dimensional interactions between Tb^{3+} ion or Eu^{3+} ions occurs, which lead to a high self-quenching concentration. The high quenching concentration of $\text{Gd}_{2-x}\text{Tb}_x\text{W}_3\text{O}_{12}$ phosphors can be attributed to the crystal structure of $\text{Gd}_2\text{W}_3\text{O}_{12}$ host. As shown in Fig. 2(b), the nearest edge-sharing $[\text{GdO}_8]$ polyhedrons form one-dimensional chains. In general, the concentration quenching of Tb^{3+} ion is due to the non-radiative

energy transfer between Tb^{3+} ions^[22-23]. Owing to the little differences between $^5\text{D}_3 \rightarrow ^5\text{D}_4$ and $^7\text{F}_6 \rightarrow ^7\text{F}_0$ of Tb^{3+} , the cross relaxation process was described as Equation (2):



Thus, Tb^{3+} ion in the excitation state of $^5\text{D}_3$ would release to a lower excitation state of $^5\text{D}_4$ and the neighboring Tb^{3+} ion in the ground state of $^7\text{F}_6$ would be excited to the excitation state of $^7\text{F}_0$. As a result, the neighboring Tb^{3+} ion act as quenching center which lead to the quenching of Tb^{3+} ion. In such one-dimensional structure, the energy transfer can lead to concentration quenching at a very high concentration.

The critical distance (R_c) between Tb^{3+} ion was calculated by the concentration quenching method, with the following formula (Eq. (3)) proposed by Blasse^[24]:

$$R_c \approx 2 \left[\frac{3V}{4\pi x_c N} \right]^{\frac{1}{3}} \quad (3)$$

where V is the volume of crystallographic unit cell, x_c is the critical concentration and N is the lattice site number in the unit cell which can be replaced by sensitizers. In $\text{Gd}_2\text{W}_3\text{O}_{12}$, $V=0.493278 \text{ nm}^3$, $N=8$, and $x_c=0.75$. The R_c of Tb^{3+} ions is thus calculated to be 0.539 nm. In general, for energy transfer process, the exchange interaction and multipole interaction are two dominant mechanisms^[25]. Exchange interactions generally take place over the dis-

tance shorter than 0.5 nm^[26]. Since the critical distance of Tb^{3+} ions in $\text{Tb}_2\text{W}_3\text{O}_{12}$ is 0.539 nm, which is close to 0.5 nm, exchange interaction is expected to play the dominant role in the energy transfer process.

Due to the red emission under NUV excitation, Eu^{3+} and Sm^{3+} ions were utilized to adjust the CIE coordinates of phosphors to yellow region. Fig. 5 (a, b) show the excitation spectra of Eu^{3+} and Sm^{3+} doped $\text{Gd}_{0.5}\text{Tb}_{1.5}\text{W}_3\text{O}_{12}$ phosphors, respectively. Since the excitation bands of Eu^{3+} and Sm^{3+} ions overlap with that of Tb^{3+} , the excitation band of Eu^{3+} or Sm^{3+} cannot be differentiated in the excitation spectra. As shown in Fig. 5 (a, b), due to the competition between Tb^{3+} and Eu^{3+} (Sm^{3+}) ions, the excitation intensities of Tb^{3+} ions decrease as doping concentration of Eu^{3+} and Sm^{3+} ions increase. The strongest excitation peaks of both Eu^{3+} and Sm^{3+} doped $\text{Gd}_{0.5-y}\text{Tb}_{1.5}\text{RE}_y\text{W}_3\text{O}_{12}$ phosphors locate at 382 nm.

Fig. 5 (c, d) show the emission spectra of $\text{Gd}_{0.5-y}\text{Tb}_{1.5}\text{RE}_y\text{W}_3\text{O}_{12}$ phosphors doped with Eu^{3+} and Sm^{3+} at 382 nm excitation. In Fig. 5 (c), there are two emission peaks at 598 and 619 nm, which correspond to the $^5\text{D}_0 \rightarrow ^7\text{F}_1$ and $^5\text{D}_0 \rightarrow ^7\text{F}_2$ transitions of Eu^{3+} ion, respectively. As the doping amount of Eu^{3+} ion increases to 0.010, the emission intensity at 619 nm increases. Yet, as the doping amount of Eu^{3+} further increases, the concentration quenching of Eu^{3+} ions occurs.

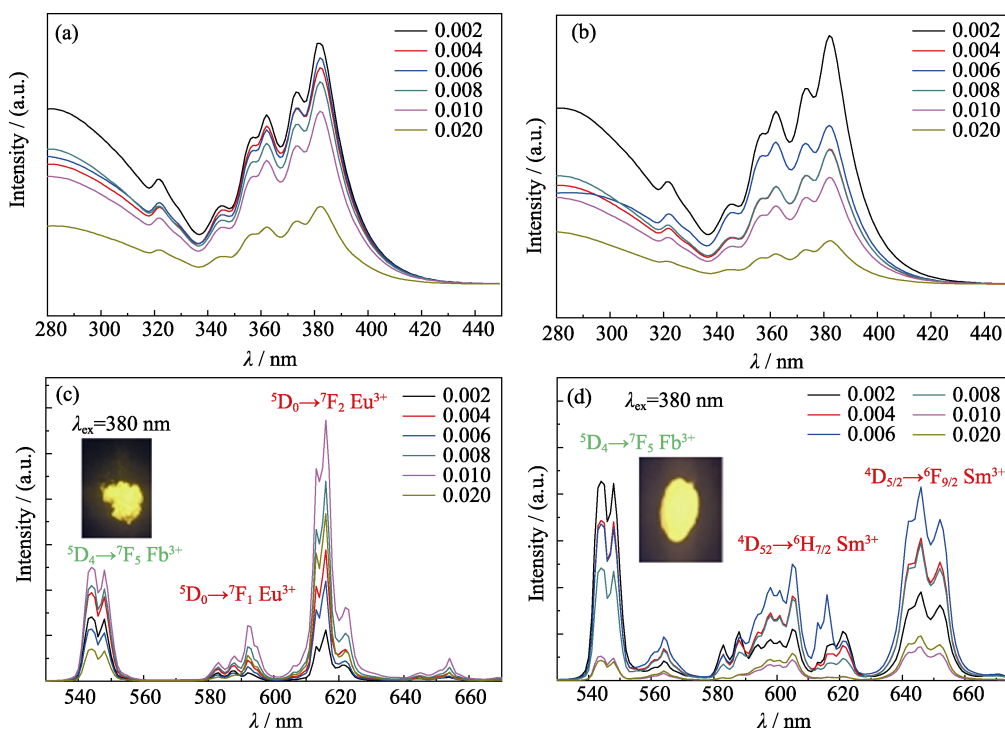


Fig. 5 (a, b) The excitation spectra of $\text{Gd}_{0.5-y}\text{Tb}_{1.5}\text{RE}_y\text{W}_3\text{O}_{12}$ (RE=Eu, Sm), (c, d) the emission spectra of $\text{Gd}_{0.5-y}\text{Tb}_{1.5}\text{RE}_y\text{W}_3\text{O}_{12}$ (RE=Eu, Sm) with 382 nm excitation
Colourful spectra are available on website

The electric dipole transition of $^5D_0 \rightarrow ^7F_2$ emission of Eu^{3+} ion belongs to the hypersensitive transition and is very sensitive to surrounding environment^[27]. In Fig. 5 (c), the electric dipole transition of $^5D_0 \rightarrow ^7F_2$ (619 nm) emission intensity is significantly stronger than the peak intensity at 598 nm, which indicates that the doping position of Eu^{3+} has no inversion center. As shown in Fig. 5(d), besides the characteristic emission of Tb^{3+} ion in 549 nm ($^5D_4 \rightarrow ^7F_5$), the emission peaks of Sm^{3+} are also present in the emission spectrum of $\text{Gd}_{0.5-y}\text{Tb}_{1.5}\text{Sm}_y\text{W}_3\text{O}_{12}$ phosphors. Those emission peaks at 610 ($^4G_{5/2} \rightarrow ^6H_{7/2}$) and 650 nm ($^4G_{5/2} \rightarrow ^6H_{9/2}$) correspond to the f-f transition of Sm^{3+} . With the increasing concentration of Sm^{3+} ion, the emission intensity of Tb^{3+} ion decrease, and Sm^{3+} ion achieved the strongest emission at the concentration of 0.3mol%. Since the emission intensity ratio of $\text{Tb}^{3+}/\text{Eu}^{3+}$ and $\text{Tb}^{3+}/\text{Sm}^{3+}$ changes with the concentration of Eu^{3+} and Sm^{3+} , the CIE coordinates of both $\text{Gd}_{0.5-y}\text{Tb}_{1.5}\text{Eu}_y\text{W}_3\text{O}_{12}$ and $\text{Gd}_{0.5-y}\text{Tb}_{1.5}\text{Sm}_y\text{W}_3\text{O}_{12}$ phosphors vary from green to yellow region. Thus, yellow light emission under NUV

light excitation is realized by adjusting the concentration of Eu^{3+} or Sm^{3+} ion in $\text{Gd}_{0.5-y}\text{Tb}_{1.5}\text{RE}_y\text{W}_3\text{O}_{12}$ (RE=Eu, Sm) phosphors.

As shown in Table 1, the IQE of both $\text{Gd}_{0.494}\text{Tb}_{1.5}\text{Eu}_{0.006}\text{W}_3\text{O}_{12}$ and $\text{Gd}_{0.494}\text{Tb}_{1.5}\text{Sm}_{0.006}\text{W}_3\text{O}_{12}$ are reasonably high, although it still needs improvement. Moreover, the synthesis of $\text{Gd}_{0.494}\text{Tb}_{1.5}\text{Eu}_{0.006}\text{W}_3\text{O}_{12}$ and $\text{Gd}_{0.494}\text{Tb}_{1.5}\text{Sm}_{0.006}\text{W}_3\text{O}_{12}$ can be performed in ambient atmosphere, as opposed to the reducing environment that Ce (III) containing compounds require. Thus, $\text{Gd}_{0.494}\text{Tb}_{1.5}\text{Eu}_{0.006}\text{W}_3\text{O}_{12}$ and $\text{Gd}_{0.494}\text{Tb}_{1.5}\text{Sm}_{0.006}\text{W}_3\text{O}_{12}$ can be used as yellow light emission phosphors to fabricate W-LED device.

2.3 CIE coordinates

The 1931 CIE chromaticity diagram of $\text{Gd}_{2-x}\text{Tb}_x\text{W}_3\text{O}_{12}$ ($x=0, 0.25, 0.75, 1.00, 1.25, 1.50, 1.75, 2.00$) and $\text{Eu}^{3+}/\text{Sm}^{3+}$ doped $\text{Gd}_{0.5-y}\text{Tb}_{1.5}\text{RE}_y\text{W}_3\text{O}_{12}$ (RE=Eu, Sm; $y=0, 0.002, 0.004, 0.006, 0.008, 0.010, 0.020$) phosphors are shown in Fig. 6 (a-c), respectively. As shown in Fig. 6(a), the 1931 CIE coordinates are constantly close to

Table 1 Comparison of the IQE and CIE coordinates of $\text{Gd}_{0.5-y}\text{Tb}_{1.5}\text{RE}_y\text{W}_3\text{O}_{12}$ (RE=Eu, Sm) with other yellow phosphors

Sample	$\lambda_{\text{ex}}/\text{nm}$	IQE	CIE coordinates (x, y)
YAG: Ce^{3+} (Nichia, Japan)	430	~90%	Yellow
$\text{Sr}_3\text{AlO}_4\text{F}: \text{Ce}^{3+}$ ^[28]	430	84%	Yellow
$\text{Gd}_3\text{Al}_2\text{Ga}_3\text{O}_{12}: \text{Ce}^{3+}$ ^[29]	435	81.9%	Yellow
$\text{La}_3\text{Si}_6\text{N}_{11}: \text{Ce}^{3+}$ ^[30]	450	78.6%	(0.422, 0.553)
$\text{LuVO}_4: \text{Bi}^{3+}$ ^[31]	305	68%	Yellow
$\text{Tb}_{2.82}\text{Ce}_{0.09}\text{Eu}_{0.09}\text{Al}_5\text{O}_{12}$ ^[32]	460	40%	Yellow
$\text{Sr}_3\text{Lu}_{0.95}\text{Ce}_{0.05}\text{Al}_2\text{O}_{7.5}$ ^[33]	450	41%	(0.454, 0.533)
$\text{Ca}_{1.5}\text{Mn}_{0.5}\text{Gd}_{7.6}\text{Ce}_{0.4}(\text{SiO}_4)_6\text{O}_2$ ^[34]	330	33.9%	(0.552, 0.423)
$\text{NaSc}_{0.75}\text{Mn}_{0.20}\text{Eu}_{0.05}\text{Si}_2\text{O}_6$ ^[35]	365	33%	(0.431, 0.465)
$\text{La}_{0.90}\text{Tb}_{0.08}\text{Eu}_{0.02}\text{NbO}_4$ ^[36]	261	30%	(0.473, 0.500)
$\text{Gd}_{0.86}\text{Eu}_{0.12}\text{Tb}_{0.02}\text{NbO}_4$ ^[37]	260	21.1%	Yellow
$\text{Gd}_{0.494}\text{Tb}_{1.5}\text{Sm}_{0.006}\text{W}_3\text{O}_{12}$ (This work)	382	47.8%	(0.510, 0.456)
$\text{Gd}_{0.494}\text{Tb}_{1.5}\text{Eu}_{0.006}\text{W}_3\text{O}_{12}$ (This work)	382	39.6%	(0.491, 0.472)

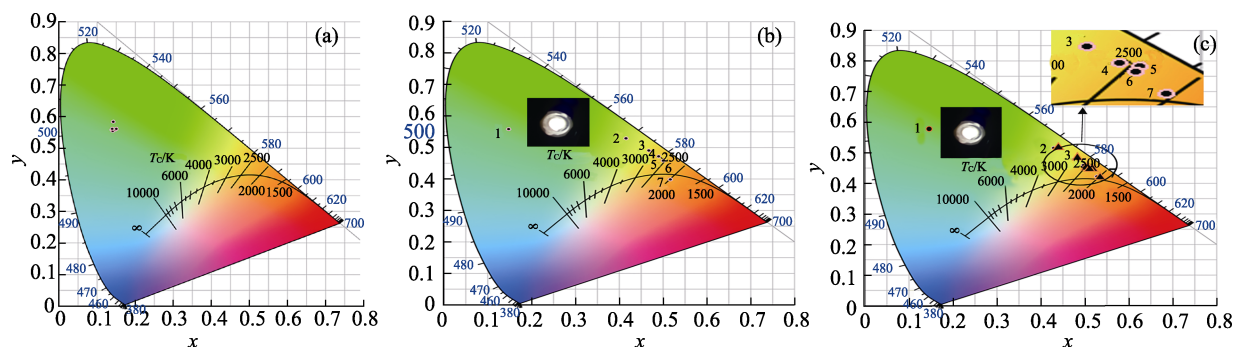


Fig. 6 The 1931 CIE coordinates diagram of (a) $\text{Gd}_{2-x}\text{Tb}_x\text{W}_3\text{O}_{12}$ ($x=0, 0.25, 0.75, 1.00, 1.25, 1.50, 1.75, \text{ and } 2.00$), (b) $\text{Gd}_{0.5-y}\text{Tb}_{1.5}\text{Eu}_y\text{W}_3\text{O}_{12}$ ($y=0, 0.002, 0.004, 0.006, 0.008, 0.010, \text{ and } 0.020$) and (c) $\text{Gd}_{0.5-y}\text{Tb}_{1.5}\text{Sm}_y\text{W}_3\text{O}_{12}$ ($y=0, 0.002, 0.004, 0.006, 0.008, 0.010, \text{ and } 0.020$). The inserts in (b) and (c) are W-LED (1W), which was fabricated by $\text{Gd}_{0.494}\text{Tb}_{1.5}\text{Eu}_{0.006}\text{W}_3\text{O}_{12}$ or $\text{Gd}_{0.494}\text{Tb}_{1.5}\text{Sm}_{0.006}\text{W}_3\text{O}_{12}$ phosphors and NUV-blue chip, respectively

Table 2 The CIE coordinates of $\text{Gd}_{0.5-y}\text{Tb}_{1.5}\text{RE}_y\text{W}_3\text{O}_{12}$ (RE=Eu, Sm)

Samples	y (Eu^{3+})	CIE coordinates (x, y)	y (Sm^{3+})	CIE coordinates (x, y)
1	0	(0.140, 0.562)	0	(0.140, 0.562)
2	0.002	(0.416, 0.529)	0.002	(0.430, 0.516)
3	0.004	(0.468, 0.490)	0.004	(0.476, 0.480)
4	0.006	(0.491, 0.472)	0.006	(0.510, 0.456)
5	0.008	(0.501, 0.459)	0.008	(0.497, 0.460)
6	0.010	(0.518, 0.444)	0.010	(0.508, 0.450)
7	0.020	(0.572, 0.400)	0.020	(0.528, 0.423)

(0.14, 0.56) with increasing concentration of Tb^{3+} . As shown in Fig. 6 (b, c), due to the emission of Eu^{3+} and Sm^{3+} ions, the introduction of both Eu^{3+} and Sm^{3+} has significant influence on the color coordinates of $\text{Gd}_{0.5-y}\text{Tb}_{1.5}\text{RE}_y\text{W}_3\text{O}_{12}$ (RE=Eu, Sm; $y=0, 0.002, 0.004, 0.006, 0.008, 0.010, 0.020$). Table 2 lists the CIE coordinates of $\text{Gd}_{0.5-y}\text{Tb}_{1.5}\text{Eu}_y\text{W}_3\text{O}_{12}$ and $\text{Gd}_{0.5-y}\text{Tb}_{1.5}\text{Sm}_y\text{W}_3\text{O}_{12}$ with different Eu^{3+} or Sm^{3+} concentration. The 1931 CIE coordinates of $\text{Gd}_{0.494}\text{Tb}_{1.5}\text{Eu}_{0.006}\text{W}_3\text{O}_{12}$ and $\text{Gd}_{0.494}\text{Tb}_{1.5}\text{Sm}_{0.006}\text{W}_3\text{O}_{12}$ are (0.491, 0.472), (0.510, 0.456), respectively, both belonging to the yellow region.

3 Conclusion

$\text{Gd}_{2-x}\text{Tb}_x\text{W}_3\text{O}_{12}$ ($x=0, 0.25, 0.5, 0.75, 1.0, 1.25, 1.50, 1.75, 2.00$) and $\text{Gd}_{0.5-y}\text{Tb}_{1.5}\text{RE}_y\text{W}_3\text{O}_{12}$ (RE=Eu, Sm; $y=0.002, 0.004, 0.006, 0.008, 0.010, 0.020$) phosphors were prepared by high temperature solid state synthesis. For the green emitting $\text{Gd}_{2-x}\text{Tb}_x\text{W}_3\text{O}_{12}$ phosphors, with very close ionic radii of Tb^{3+} with Gd^{3+} , the doping can be tuned in the entire concentration range, allowing the access to the optimum IQE of 37.6%. $\text{Gd}_{0.494}\text{Tb}_{1.5}\text{Eu}_{0.006}\text{W}_3\text{O}_{12}$ and $\text{Gd}_{0.494}\text{Tb}_{1.5}\text{Sm}_{0.006}\text{W}_3\text{O}_{12}$ emit bright yellow light under the excitation at 382 nm. The IQE of 47.8% for $\text{Gd}_{0.494}\text{Tb}_{1.5}\text{Sm}_{0.006}\text{W}_3\text{O}_{12}$ is reasonably high. $\text{Gd}_{0.494}\text{Tb}_{1.5}\text{Eu}_{0.006}\text{W}_3\text{O}_{12}$ and $\text{Gd}_{0.494}\text{Tb}_{1.5}\text{Sm}_{0.006}\text{W}_3\text{O}_{12}$ were used for the fabrication of W-LEDs pumped by NUV LED chips. Thus, $\text{Gd}_{0.494}\text{Tb}_{1.5}\text{Eu}_{0.006}\text{W}_3\text{O}_{12}$ and $\text{Gd}_{0.494}\text{Tb}_{1.5}\text{Sm}_{0.006}\text{W}_3\text{O}_{12}$ are candidates for yellow emitting phosphors. Additionally, the full-range doping strategy can be used in other systems for obtaining high quantum efficiency.

References:

- [1] CRAWFORD M H. LEDs for solid-state lighting: Performance challenges and recent advances. *IEEE Journal of Selected Topics in Quantum Electronics*, 2009, **15**(4): 1028–1040.
- [2] SHANG M, LI C, LIN J. How to produce white light in a single-phase host? *Chemical Society Reviews*, 2014, **43**(5): 1372–1386.
- [3] ZHOU J, XIA Z. Luminescence color tuning of Ce^{3+} , Tb^{3+} and Eu^{3+} codoped and tri-doped $\text{BaY}_2\text{Si}_3\text{O}_{10}$ phosphors via energy transfer. *Journal of Materials Chemistry C*, 2015, **3**(29): 7552–7560.
- [4] YANG P K, CHEN J C, CHUANG Y H. Improvement on reflective color measurement using a tri-color LED by multi-point calibration. *Optics Communications*, 2007, **272**(2): 320–324.
- [5] PARK J K, KIM C H, PARK S H, *et al.* Application of strontium silicate yellow phosphor for white light-emitting diodes. *Applied Physics Letters*, 2004, **84**(10): 1647–1649.
- [6] SONG G, MIAO J, JIANG B, *et al.* White LED based on near UV LED chip precoated with tri-color phosphors. *Semiconductor Technology*, 2011, **36**(8): 586–590.
- [7] YE S, XIAO F, PAN Y X, *et al.* Phosphors in phosphor-converted white light-emitting diodes: recent advances in materials, techniques and properties. *Materials Science and Engineering: R: Reports*, 2010, **71**(1): 1–34.
- [8] LIU Y, SILVER J, XIE R J, *et al.* An excellent cyan-emitting orthosilicate phosphor for NUV-pumped white LED application. *Journal of Materials Chemistry C*, 2017, **5**(2): 12365–12377.
- [9] LIU Y, ZHANG J, ZHANG C, *et al.* $\text{Ba}_9\text{Lu}_2\text{Si}_6\text{O}_{24}:\text{Ce}^{3+}$: an efficient green phosphor with high thermal and radiation stability for solid-state lighting. *Advanced Optical Materials*, 2015, **3**(8): 1096–1101.
- [10] LIN C C, TANG Y S, HU S F, *et al.* $\text{KBaPO}_4:\text{Ln}$ (Ln=Eu, Tb, Sm) phosphors for UV excitable white light-emitting diodes. *Journal of Luminescence*, 2009, **129**(12): 1682–1684.
- [11] LI P, WANG Z, YANG Z, *et al.* Luminescent characteristics of $\text{LiCaBO}_3:\text{M}$ (M= Eu^{3+} , Sm^{3+} , Tb^{3+} , Ce^{3+} , Dy^{3+}) phosphor for white LED. *Journal of Luminescence*, 2010, **130**(2): 222–225.
- [12] TIAN Y, CHEN B, HUA R, *et al.* Co-precipitation synthesis and characterization of Bi^{3+} , Eu^{3+} co-doped nanocrystal Gd_2WO_6 phosphors. *J. Nanosci Nanotechnol*, 2010, **10**(3): 1943–1946.
- [13] ZOU Z, WU T, LU H, *et al.* Structure, luminescence and temperature sensing in rare earth doped glass ceramics containing $\text{NaY}(\text{WO}_4)_2$ nanocrystals. *RSC Advances*, 2018, **8**(14): 7679–7686.
- [14] LI J, LI J G, LIU S, *et al.* Greatly enhanced Dy^{3+} emission via efficient energy transfer in gadolinium aluminate garnet ($\text{Gd}_3\text{Al}_5\text{O}_{12}$) stabilized with Lu^{3+} . *Journal of Materials Chemistry C*, 2013, **1**(45): 7614–7622.
- [15] SHANNON R D. Revised effective ionic radii and systematic studies of interatomic distances in halides and chalcogenides. *Acta Crystallographica, Section A: Crystal Physics, Diffraction, Theoretical and General Crystallography*, 1976, **32**(5): 751–767.
- [16] LEI, BINGFU, SHI-QING, *et al.* Luminescence properties of Sm^{3+} -doped $\text{Sr}_3\text{Sn}_2\text{O}_7$ phosphor. *Materials Chemistry & Physics*, 2010, **124**(2): 912–915.
- [17] YU R, NOH H M, MOON B K, *et al.* Photoluminescence characteristics of Sm^{3+} -doped Ba_2CaWO_6 as new orange-red emitting phosphors. *Journal of Luminescence*, 2014, **152**(5): 133–137.
- [18] JAIN A, SHYUE PING O, HAUTIER G, *et al.* Commentary: The Materials Project: a materials genome approach to accelerating materials innovation. *APL Materials*, 2013, **1**(1): 011002.

- [19] HOU Z, CHENG Z, LI G, *et al.* Electrospinning-derived $\text{Tb}_2(\text{WO}_4)_3$: Eu^{3+} nanowires: energy transfer and tunable luminescence properties. *Nanoscale*, 2011, **3**(4): 1568–1574.
- [20] RAI V K, RAI S B, RAI D K. Optical properties of Tb^{3+} doped tellurite glass. *Journal of Materials Science Letter*, 2004, **39**(15): 4971–4975.
- [21] FOUASSIER C, SAUBAT B, HAGENMULLER P. Self-quenching of Eu^{3+} and Tb^{3+} luminescence in $\text{LaMgB}_5\text{O}_{10}$: a host structure allowing essentially one-dimensional interactions. *Journal of Luminescence*, 1981, **23**(3): 405–412.
- [22] DU Z, LIU Q, HOU T, *et al.* The effects of Tb^{3+} doping concentration on luminescence properties and crystal structure of BaF_2 phosphor. *Bulletin of Materials Science*, 2015, **38**(3): 1–5.
- [23] LIU Y, ZHANG J, ZHANG C, *et al.* High efficiency green phosphor $\text{Ba}_9\text{Lu}_2\text{Si}_6\text{O}_{24}:\text{Tb}^{3+}$: visible quantum cutting via cross-relaxation energy transfers. *Journal of Physical Chemistry C*, 2016, **120**(4): 2362–2370.
- [24] BLASSE G. Energy transfer in oxionic phosphors. *Physics Letters A*, 1968, **28**(6): 444–445.
- [25] VAN UITERT L G, JOHNSON L F. Energy transfer between rare-earth ions. *The Journal of Chemical Physics*, 1966, **44**(9): 3514–3522.
- [26] DEXTER D L, SCHULMAN J H. Theory of concentration quenching in inorganic phosphors. *Journal of Chemical Physics*, 1954, **22**(6): 1063–1070.
- [27] QIANG S. Influence of environment on the luminescence of rare earths. *Journal of Luminescence*, 1988, **40–41**: 113–114.
- [28] ZHENG X, LUO H, LIU J, *et al.* $\text{Sr}_3\text{AlO}_4\text{F}:\text{Ce}^{3+}$ -based yellow phosphors: structural tuning of optical properties, and use in solid-state white lighting. *Journal of Materials Chemistry C*, 2013, **1**(45): 7598–7607.
- [29] LIU Y F, LIU P, WANG L, *et al.* A two-step solid-state reaction to synthesize the yellow persistent $\text{Gd}_3\text{Al}_2\text{Ga}_3\text{O}_{12}:\text{Ce}^{3+}$ phosphor with an enhanced optical performance for AC-LEDs. *Chemical Communications*, 2017, **53**(53): 10636–10639.
- [30] DU F, ZHUANG W, LIU R, *et al.* Synthesis, structure and luminescent properties of yellow phosphor $\text{La}_3\text{Si}_6\text{N}_{11}:\text{Ce}^{3+}$ for high power white-LEDs. *Journal of Rare Earths*, 2017, **35**(11): 1059–1064.
- [31] FENGWEN K, MINGYING P, QINYUAN Z, *et al.* Abnormal anti-quenching and controllable multi-transitions of Bi^{3+} luminescence by temperature in a yellow-emitting $\text{LuVO}_4:\text{Bi}^{3+}$ phosphor for UV-converted white LEDs. *Chemistry-A European Journal*, 2015, **20**(36): 11522–11530.
- [32] NAZAROV M, NOH D Y, SOHN J, *et al.* Quantum efficiency of double activated $\text{Tb}_3\text{Al}_5\text{O}_{12}:\text{Ce}^{3+}, \text{Eu}^{3+}$. *Journal of Solid State Chemistry*, 2007, **180**(9): 2493–2499.
- [33] TAO Z, ZHANG W, QIN L, *et al.* A yellow-emitting nanophosphor of Ce^{3+} -activated aluminate $\text{Sr}_3\text{LuAl}_2\text{O}_{7.5}$. *Journal of Alloys & Compounds*, 2014, **588**(5): 540–545.
- [34] LI G, GENG D, SHANG M, *et al.* Tunable luminescence of $\text{Ce}^{3+}/\text{Mn}^{2+}$ -coactivated $\text{Ca}_2\text{Gd}_8(\text{SiO}_4)_6\text{O}_2$ through energy transfer and modulation of excitation: potential single-phase white/yellow-emitting phosphors. *Journal of Materials Chemistry*, 2011, **21**(35): 13334–13344.
- [35] XIA Z, ZHANG Y, MOLOKEEV M S, *et al.* Structural and luminescence properties of yellow-emitting $\text{NaScSi}_2\text{O}_6:\text{Eu}^{2+}$ phosphors: Eu^{2+} site preference analysis and generation of red emission by codoping Mn^{2+} for white-light-emitting diode applications. *Journal of Physical Chemistry C*, 2013, **117**(40): 20847–20854.
- [36] LI K, ZHANG Y, LI X, *et al.* Host-sensitized luminescence in $\text{LaNbO}_4:\text{Ln}^{3+}$ ($\text{Ln}^{3+} = \text{Eu}^{3+}/\text{Tb}^{3+}/\text{Dy}^{3+}$) with different emission colors. *Physical Chemistry Chemical Physics*, 2015, **17**(6): 4283–4292.
- [37] LIU X, CHEN C, LI S, *et al.* Host-sensitized and tunable luminescence of $\text{GdNbO}_4:\text{Ln}^{3+}$ ($\text{Ln}^{3+} = \text{Eu}^{3+}/\text{Tb}^{3+}/\text{Tm}^{3+}$) nanocrystalline phosphors with abundant color. *Inorganic Chemistry*, 2016, **55**(20): 10383–10396.

全范围掺杂调制强黄色发光 $\text{Gd}_{0.5-y}\text{Tb}_{1.5}\text{RE}_y\text{W}_3\text{O}_{12}$ (RE=Eu, Sm) 荧光粉的研究

代艳南¹, 杨 帅¹, 沈 阳², 单永奎¹, 杨 帆¹, 赵庆彪²

(华东师范大学 1. 化学与分子工程学院; 2. 光信息科学与工程系, 极化材料与器件教育部重点实验室, 上海 200241)

摘 要: 黄光荧光材料在近紫外(NUV)芯片激发的白光发光二极管(W-LED)的制造中起重要作用。在本研究中, 通过在 $\text{Gd}_2\text{W}_3\text{O}_{12}$ 基质中共掺 $\text{Tb}^{3+}/\text{Eu}^{3+}$ 或 $\text{Tb}^{3+}/\text{Sm}^{3+}$, 从而获得较强的黄光发射。由于 Gd^{3+} 的有效激发通常在深紫外区, 在 $\text{Gd}_2\text{W}_3\text{O}_{12}$ 中并不会被 382 nm 的紫外光激发, 因此 Gd^{3+} 对 $\text{Tb}^{3+}/\text{Eu}^{3+}$ 、 $\text{Tb}^{3+}/\text{Sm}^{3+}$ 共掺杂的黄光发射并无影响。而 Tb^{3+} 与 Gd^{3+} 具有相似的离子半径, Tb^{3+} 在全浓度范围内可以对 Gd^{3+} 进行取代。当 Tb^{3+} 离子掺杂浓度为 75mol% 时, 该体系绿光的发射强度达到最强, 对应的内量子产率(IQE)为 37.6%。在最佳 Tb^{3+} 掺杂浓度下, 通过引入可以被近紫外光有效激发的 Eu^{3+} 或 Sm^{3+} , 在 $\text{Gd}_2\text{W}_3\text{O}_{12}$ 基质中实现 $\text{Tb}^{3+}/\text{Eu}^{3+}$ 或 $\text{Tb}^{3+}/\text{Sm}^{3+}$ 共同掺杂, 得到了高亮度的黄色发光, IQE 分别达到 39.6% 和 47.8%。利用制备的 $\text{Gd}_{0.494}\text{Tb}_{1.5}\text{Eu}_{0.006}\text{W}_3\text{O}_{12}$ 和 $\text{Gd}_{0.494}\text{Tb}_{1.5}\text{Sm}_{0.006}\text{W}_3\text{O}_{12}$ 黄光荧光粉与 NUV-蓝色芯片成功组装了 W-LED 器件。由此可见, $\text{Gd}_{0.5-y}\text{Tb}_{1.5}\text{RE}_y\text{W}_3\text{O}_{12}$ (RE=Eu, Sm) 荧光粉有望用于组装 W-LED 器件。此外, 全范围掺杂法可用于其他体系以获得高效的荧光粉。

关 键 词: 固相合成; 荧光; 钨酸盐; 稀土; 内量子效率

中图分类号: TQ174 文献标识码: A